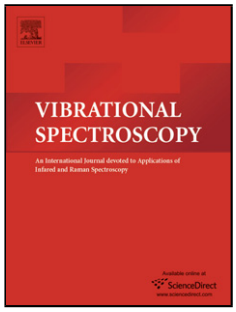


Title: A conformational study of hydroxylated isoflavones by vibrational spectroscopy coupled with DFT calculations

Author: N.F.L. Machado L.A.E. Batista de Carvalho J.C. Otero M.P.M. Marques

PII: S0924-2031(13)00106-9
DOI: http://dx.doi.org/doi:10.1016/j.vibspec.2013.08.010
Reference: VIBSPE 2256

To appear in: *VIBSPE*

Received date: 6-3-2013
Revised date: 20-8-2013
Accepted date: 21-8-2013

Please cite this article as: N.F.L. Machado, L.A.E.B. Carvalho, J.C. Otero, M.P.M. Marques, A conformational study of hydroxylated isoflavones by vibrational spectroscopy coupled with DFT calculations, *Vibrational Spectroscopy* (2013), http://dx.doi.org/10.1016/j.vibspec.2013.08.010

# A conformational study of hydroxylated isoflavones by vibrational spectroscopy coupled with DFT calculations

N.F.L. Machado[a], L.A.E. Batista de Carvalho[a], J.C. Otero[b], M.P.M. Marques[a,c,*]

[a] *Research Unit "Molecular Physical-Chemistry", University of Coimbra – Rua Larga 3005-535, Coimbra, Portugal*

[b] *Department of Physical-Chemistry, Faculty of Science, University of Malaga – Campus de Teatinos, 29071, Málaga, Spain*

[c] *Department of Life Sciences, Faculty of Science and Technology, University of Coimbra – Ap 3046, 3301-401, Coimbra, Portugal*

**Abstract**

The conformational preferences of a series of hydroxylated isoflavones were studied by optical vibrational spectroscopy (FTIR and Raman) coupled with density functional theory (DFT) calculations. Special attention was paid to the effect of the hydroxyl substitution, due to the importance of this group in the biological activity of these systems. The isoflavones investigated – daidzein, genistein and formononetin – were shown to exist in distinct conformations in the solid state, namely regarding the orientation of the hydroxylic groups at $C^7$ and within the catechol moiety, that are determinant factors for their conformational behaviour and antioxidant ability. In the light of the most stable conformers obtained for each molecule, a complete assignment of their experimental vibrational spectra was performed.

*Keywords:* Phytochemicals; Isoflavones; Chemoprevention; Raman; FTIR; DFT calculations

## 1. Introduction

* Corresponding author. Tel.: +351 239826541, Fax: +351 239826541;
E-mail address: pmc@ci.uc.pt (M.P.M. Marques).

Phytochemicals are a class of compounds comprising a wide variety of molecules present in plants, including flavonoids which are known to possess significant health-promoting properties, generally related with their capabilities to act as chain-breaking antioxidants or as radical scavengers [1, 2]. In fact, oxidative stress occurs upon disruption of the homeostatic balance between free radical generation and the natural antioxidant defence mechanisms (*e.g.* by glutathione and regulatory enzymes such as superoxide dismutase, catalase and peroxidases). This is recognised to be directly linked to damage in numerous cell targets (DNA, lipids and proteins) and may therefore lead to severe pathologies such as cardiovascular and neurodegenerative disorders or even cancer. Thus, dietary habits play a key role in the prevention of these diseases since the intake of phytochemicals through the diet, in appropriate amounts, may help to maintain the homeostatic oxidative balance [3].

In the last decade the beneficial properties of phytochemicals have led to a vigorous search for novel antioxidants from natural sources, involving the nutritional, pharmacological and medicinal chemistry fields [3-16], with particular emphasis on the prevention of cancer and cardiovascular disorders through the consumption of these kind of nutraceuticals in the daily diet [17-20]. Accordingly, special attention has been paid to phenolic acids, anthocyanins, coumarins, tannins and flavonoids (including flavones and isoflavones), the latter constituting the largest group among phytochemicals [21].

Besides the well-established role in the defence mechanisms against oxidative processes, either from deleterious radical species or from UV radiation, assigned to isoflavones, an important estrogen-mimicking effect has been also recognised to this specific family of compounds [22, 23]. Furthermore, a wide variety of other pharmacologically relevant functions have been assigned to these dietary phenols, from antibacterial, antiviral, anti-inflammatory and anti-HIV to anticancer [18, 24,

25]. This group of compounds contains a common moiety – a chromone skeleton with a phenyl substituent at position 3 (Fig. 1) – which is greatly responsible for their biological role. However, this is also determined by other structural parameters, such as the number and position of the hydroxyl ring substituent groups, as well as their relative orientation [24, 26, 27]. In fact, a single variation in one of these factors can induce a considerable change of their biological activity and therefore of their medicinal role. Additionally, this substitution profile rules the conformational behaviour of the systems, namely their flexibility, the formation of hydrogen bonds – either intra- or intermolecularly – and the occurrence of planar or skewed relative orientations of the pendant groups. Therefore, the beneficial activity of the isoflavones under study relies on their structural and conformational preferences [28-31]. Besides determining biological activity, these strict structure-activity relationships (SAR´s) modulate the distribution and bioavailability of the compounds within the cell.

Consequently, it is essential to have an accurate conformational knowledge of these kind of phytochemical systems, which can be attained through the combined use of spectroscopic techniques and theoretical approaches. This will lead to a better understanding of their mechanisms of action, and will enable to establish reliable SAR´s, crucial for a rational design of effective bioactive compounds based on these natural products. In the present work, the conformational preferences of a series of isoflavones, with different substitution patterns, were studied by Raman and Fourier transform infrared (FTIR) spectroscopies coupled with density functional theory (DFT) calculations. The FTIR technique assumes special importance in the study of these kind of hydroxylated systems, due to its responsiveness in the detection of the vibrational modes related to the OH groups (*e.g.* stretching and bending modes),

which yield relevant information on the conformational preferences in the molecules, closely associated to their biological function.

Three compounds were investigated – 4´,7-dihydroxyisoflavone (daidzein, DAID), 4´,5,7-trihydroxyisoflavone (genistein, GEN) and 7-hydroxy-4´-methoxyisoflavone (formononetin, FOR) (Fig. 1). The results thus obtained are related to the free radical scavenging ability of the compounds, previously assessed by the authors [29].

*Figure 1*

## 2. Materials and methods

### *2.1. Chemicals*

Daidzein (97%) and genistein (97%) were purchased from Alfa Aesar (Lancashire, United Kingdom). Formononetin (≥98%) was obtained from Sigma-Aldrich Química S.A. (Sintra, Portugal).

### *2.2. FTIR Spectroscopy*

The FTIR spectra were recorded in a Bruker Optics Vertex 70 FTIR spectrometer, in the 400-4000 $cm^{-1}$ range, in KBr disks (*ca.* 1% *(w/w)*). A KBr beamsplitter and a liquid nitrogen cooled Mercury Cadmium Telluride (MCT) detector were used. The spectra were collected for 2 minutes, with 2 $cm^{-1}$ resolution. The error in the peak positions was estimated to be less than 1 $cm^{-1}$.

### *2.3. Raman Spectroscopy*

The Raman spectra of DAID and FOR were obtained in a triple monochromator Jobin-Yvon T64000 Raman system (focal distance 0.640 m, aperture f/7.5) equipped

with holographic gratings of 1800 grooves.mm$^{-1}$. The premonochromator stage was used in the subtractive mode. The detection system was a liquid nitrogen cooled non-intensified 1024x256 pixel (1") charge coupled device (CCD) chip. A 90º geometry between the incident radiation and the collecting system was employed. The entrance slit was set to 200 ! m, while the slit between the premonochromator and the spectrograph was set to 400 ! m. Under the above mentioned conditions, the error in wavenumbers was estimated to be within 1 cm$^{-1}$. The 514.5 nm line of an $Ar^+$ laser (Coherent, model Innova 300-05) was used as the excitation radiation, providing *ca.* 30 mW at the sample position.

Due to the high intrinsic fluorescence of GEN, its Raman spectrum was registered in a RFS 100/S Bruker Fourier transform Raman (FT-Raman) spectrometer, with a 180º geometry, equipped with an InGaAs detector. Near-infrared excitation was provided by the 1064 nm line of a Nd:YAG laser (Coherent, model Compass-1064/500N), yielding *ca.* 250 mW at the sample position, and the resolution was set to 2 cm$^{-1}$.

In all cases, samples were sealed in Kimax glass capillary tubes of 0.8 mm inner diameter, and the spectra were obtained at room temperature.

### *2.4. Quantum mechanical calculations*

Quantum mechanical calculations were performed using the GAUSSIAN03W program [32] within the density functional theory (DFT) approach, in order to properly account for the electron correlation effects which are particularly important for these kind of conjugated systems. The widely employed hybrid method denoted by B3LYP, which includes a mixture of HF and DFT exchange terms and the gradient-corrected correlation functional of Lee, Yang and Parr [33,34], as proposed and parameterised by Becke [35,36], was used, along with the double-zeta split

valence basis set 6-31G** [37]. Molecular geometries were fully optimised by the Berny algorithm, using redundant internal coordinates [38]: the bond lengths to within *ca.* 0.1 pm and the bond angles to within *ca.* 0.1º. The final root-mean-square (rms) gradients were always less than $3 \times 10^{-4}$ Hartree.Bohr$^{-1}$ or Hartree.radian$^{-1}$, respectively. No geometrical constraints were imposed on the molecules under study. The relative energies and populations (Boltzmann distribution, at 298.15 K) were calculated for all conformers, using the sum of the electronic and zero-point energies (ZPE).

The harmonic vibrational wavenumbers, as well as the infrared and Raman activities were always obtained at the same level of theory as the geometry optimisation. Given that the widely used Merrick´s [39] scale factors do not adequately reproduce the experimental wavenumbers for these highly unsaturated chemical systems, a set of four different factors proposed by the authors for chromone derivatives was used [40]: 1.18, for the low wavenumber region (below 175 cm$^{-1}$); 1.05, from 175 to 400 cm$^{-1}$; 0.985, for the interval between 400 and 1500 cm$^{-1}$; and 0.957, above 3000 cm$^{-1}$; for the frequency range between 1500 and 1850 cm$^{-1}$, the previously proposed [39] scale factor of 0.9614 was applied.

The Raman intensities, straightforwardly derived from the program output, cannot be compared directly with the experiment, the expression relating the Raman differential scattering cross section with the Raman activity being [41],

$$\frac{\partial \sigma_i}{\partial \Omega} = \frac{(2\pi)^4}{45}(\nu_0 - \nu_i)^4 \frac{h}{8\pi^2 c \nu_i B_i} S_i. \qquad (1)$$

where $h$, $k$, $c$ and $T$ represent the Planck and Boltzmann constants, the speed of light and the temperature (in Kelvin), respectively; $\nu_0$ and $\nu_i$ stand for the frequency of the laser excitation, and the normal mode frequencies; and $B_i$ is a temperature factor, set to 1. The frequency of the laser excitation, for a 514.5 nm line of an $Ar^+$ laser, was

considered to be 19436 $cm^{-1}$. The theoretical Raman intensity was calculated according to

$$I = C(\nu_0 - \nu_i)^4 \frac{S_i}{\nu_i} \quad (2)$$

*C* being a constant. In order to simulate the linewidth of the experimental lines, an artificial Lorentzian broadening was introduced using the SWizard program (revision 4.6) [42,43]. The band half-widths were considered to be equal to 10 $cm^{-1}$.

## 3. Results and discussion

### *3.1. Conformational analysis*

A full conformational analysis was undertaken for the compounds under study, through DFT calculations. Table S1 (Supplementary material) comprises the most relevant geometrical parameters calculated for these isoflavones, while Table 1 summarises the most significant dihedral angles defining the lowest energy geometries.

DAID and GEN, both possessing a phenol group, have a similar substitution pattern except for the presence of the 5-hydroxyl in the latter (Fig. 1). In molecules containing a phenolic moiety, the hydroxyl group located in the B-ring tends to adopt a *syn* orientation relative to the carbonyl group, with the maximum stability being reached for a conformation with both the $C^7$–OH and the $C^{4'}$–OH groups displaying a *syn* orientation relative to the carbonyl (Fig. 1). In turn, a geometry with an opposite orientation (*anti*) of both these hydroxylic groups will be the most unfavoured (Table 1).

Four evenly populated conformers occur for FOR, the most unfavoured one having an energy difference smaller than 1 $kJ.mol^{-1}$ relative to the most stable species (Table 1). Apart from the methoxyl substitution in position $C^{4'}$, the FOR molecule

presents a structure and conformational behaviour similar to that of DAID. Rotation around the $C^{7}$–OH bond is responsible for a slight destabilisation (0.22 kJ.mol$^{-1}$, the same value as for DAID), while a distinct arrangement of the methoxyl group leads to a 0.61 kJ.mol$^{-1}$ energy increase relative to the most stable conformer (less than the 0.95 kJ.mol$^{-1}$ corresponding to the $C^{4'}$–OH rotation in DAID, Table 1).

The presence of a hydroxyl group at position 5 ($C^{5}$–OH) for GEN allows the formation of a quite strong (C=)O···H(O–$C^{5}$) intramolecular interaction (Fig. 1). This H-type close contact yields a six-membered ring responsible for an enhanced electronic delocalisation, which stabilises the molecular structure in highly delocalised electronic systems such as these isoflavones. This interaction has been extensively studied spectroscopically, being admittedly stronger than the H-bond between ($O^{3}$H) and the ketonic oxygen occurring in flavonols [44], that gives rise to a five-membered intramolecular ring instead. In fact, disruption of this intramolecular ($C^{5}$–OH···O) interaction is highly unfavoured: an energy value of *ca.* 63.5 kJ.mol$^{-1}$ was found between the most stable structures with and without this H-bond.

Four distinct conformers were obtained for GEN, displaying this ($C^{5}$–OH···O) interaction, with similar relative energies (Table 1). Among these, those originated by rotation around the ($C^{7}$–O) or ($C^{4'}$–O) bonds present energy differences smaller than 2.0 kJ.mol$^{-1}$ as compared to the most stable species ($\Delta E$=0.83 kJ.mol$^{-1}$ and $\Delta E$=1.99 kJ.mol$^{-1}$, respectively, Table 1). However, these energy gaps are larger than those found for DAID, since this compound is more sensitive to structural changes due to the enhanced electronic delocalisation and the presence of the stabilising 6-membered intramolecular ring.

The theoretical DFT geometries obtained for the isolated molecules under study were compared to the X-ray crystallographic data found in the literature for similar systems [45, 46], a very good agreement having been found both for bond distances

and angles. The calculated distance for the H-bond involving the ($C^5$–OH) moiety in GEN is 166 pm (Fig. 1), close to the experimental value reported for the genistein-morpholine complex (GMC, 165 pm) in the condensed phase (Table 2) [45]. Moreover, in GEN the $C^5$–O and $C^4$=$O^{12}$ distances are predicted to be 133.6 and 125.2 pm, respectively, very close to the crystallographic values of 135.9 and 126.3 pm obtained for GMC (Table 2). Regarding the most important angles, the crystallographic values of 119.4 and 153.6º for the ($C^{8a}O^1C^2$) and ($O^5H\cdots O^{12}$) angles, respectively, compare well with those calculated (119.5 and 150.3º, Table 2), once again reflecting the good quality of the structures presently obtained by DFT theoretical methods.

Regarding the aforementioned ($C^{8a}O^1C^2$) bond angle, a remarkable feature can be observed in these systems: the value of 118.5º, obtained for 7-ethoxy-formononetin (EFOR) by crystallography [46], is very close to 118.8º calculated for both DAID and FOR, while presenting a slight difference from the 119.4º value reported for GMC (Table 2). Concomitantly, the values of 126.3 and 123.1 pm measured for the $C^4$=$O^{12}$ bond for GMC and EFOR, respectively, can be compared to the larger calculated value of 125.2 pm for GEN, evidencing the distinct chemical nature of this molecule, due to the six-membered intramolecular ring (Fig. 1, Table 2).

Isoflavones are known to assume non-planar conformations [47], due to the steric hindrance between the aromatic B-ring hydrogen atoms and $C^2$(H) (Fig. 1). The predited values for ψ (that defines the rotation of ring B relative to the chromone skeleton) vary from 141.3º (GEN) to 142.7º (FOR). When compared to the crystallographic data reported for GMC and EFOR – 116.2 and 137.0º, respectively (Table 2) – the agreement between FOR and EFOR is quite good. Interestingly, this structural feature (relative orientation of ring B) may change with the solid state

crystalline packing mode, thus being strongly dependent on the compound´s substitution pattern.

In summary, the DFT calculations have shown that GEN, displaying a strong (stabilising) intramolecular close contact, has a somewhat distinct chemical nature than DAID and FOR, even though the three molecules belong to the same family. The presently obtained conformations for GEN, DAID and FOR were found to be in good accordance with previously reported X-ray data for similar compounds. Furthermore, the crystallographic structures previously gathered for GMC and EFOR [45, 46] corroborate the differences between GEN and the other two studied isoflavones, which seem to be well reproduced by the DFT calculated data.

### *3.2. Spectral Analysis*

#### *3.2.1. The 3500-2500 $cm^{-1}$ region*

Despite the high amount of spectroscopic work to be found in the literature for isoflavones, mainly by Raman and SERS (Surface Enhanced Raman Spectroscopy) techniques [48-50], a complete and accurate assignment of their vibrational spectra has not yet been achieved. Additionally, although infrared spectroscopy has a huge potential for the analysis of these polyhydroxylated compounds [44, 51, 52] no conclusive studies have been reported to date.

A detailed vibrational analysis of the DAID, GEN and FOR isoflavones was presently carried out, in combination with suitable DFT methods. Table S2 (Supplementary material) comprises all the calculated vibrational data (wavenumbers and intensities) for these compounds. The main spectral bands were assigned and compared with a view to discriminate the features common to all three compounds from those typical of each isoflavone, thus enabling a future identification of these systems by vibrational spectroscopy, a quick and reliable technique for this purpose.

In the high frequency region, the ν(CH) modes give rise to the most intense (quite sharp) bands in the Raman spectra (between 3000 and 3100 $cm^{-1}$, Fig. 2). In FTIR, in turn, these modes usually yield weak features, often partially overruled by the broad, very intense, ν(OH) bands (Fig. 3). An accurate assignment of these features is not straightforward in these systems, the most intense Raman bands within this region being originated by vibrational modes from rings A or B, or even from the $C^2H$ group (Fig. 2, Table 3).

*Figure 2*

*Figure 3*

Furthermore, the presence of different substitution patterns in the compounds investigated is responsible for distinct electronic distributions, causing marked changes in their vibrational profile, namely regarding the ν(CH) modes (Table 3). In the case of FOR, besides the characteristic vibrational features due to the ($OCH_3$) moiety, clearly visible between 2800 and 2900 $cm^{-1}$ in both the Raman and FTIR spectra (Fig. 2, Table 3), the presence of this methoxyl as a substituent of B-ring (Fig. 1) seems to shift the other ν(CH) bands to lower frequencies, probably due to the mesomeric effect exerted by the methoxy group. This is evidenced by the deviation of the signal ascribed to the ν(CH) B modes, common to all isoflavones, that occurs at *ca.* 3020 $cm^{-1}$ for both DAID and GEN, and at 2993 $cm^{-1}$ for FOR (Table 3).

The OH stretching modes, also comprised in this high frequency spectral interval, contain important information on the conformational preferences of the hydroxyl groups, as well as on their involvement in hydrogen close contacts. GEN is a good example of this, as the intense and extremely broad signal detected between 2500 and 3400 $cm^{-1}$ is due to the strong intramolecular interaction involving the ($C^5$–OH) substituent, yielding a characteristic feature in the FTIR spectra of 5-

hydroxylated chromones [52]. Two distinct infrared patterns were obtained for the ν(OH) modes: (i) a single strong broad band at about 3200 $cm^{-1}$ for DAID and at 3130 $cm^{-1}$ for FOR (with a lower intensity) (Fig. 3). (ii) a strong narrow signal at 3410 $cm^{-1}$ (detected both in Raman and FTIR) and a broad band between 2750 and 3250 $cm^{-1}$ (due to the H-bonded ($O^5H$)) observed for GEN (Figs. 2 and 3).

Furthermore, the presence of the ($O^7H$) and ($O^{4'}H$) stretching modes at higher frequencies (*ca.* 3400 $cm^{-1}$) in GEN, coupled to its sharp profile, clearly reflect non-hydrogen-bonded hydroxylic groups, which is easily justified by the preference for the strong intramolecular interaction involving the ($O^5H$) hydroxyl and the ketonic moiety. When the carbonyl group is free, in turn, it probably forms intermolecular H-bonds, which explains the lower frequency at which ν($O^7H$) and ν($O^{4'}H$) modes are detected for both DAID and FOR (Table 3).

*3.2.2. The 1750-1550 $cm^{-1}$ region*

In the 1750-1550 $cm^{-1}$ spectral region, the frequency deviations of the carbonyl stretching mode reflect the nature of the interactions in which this group is involved, therefore providing important information on the hydrogen bonding profile in this type of compounds. The ν($C^4$=$O^{12}$) and ν($C^2C^3$) modes appear in the same range, as well as deformations of the aromatic ring and the hydroxylic groups. In the case of the ($C^5$–OH) substituted GEN, the strong coupling between ν(C=O) and the aromatic ring deformations is due to the presence of the 6-membered ring formed upon (C=)O···H($O^5$) intramolecular bonding (Fig. 1, Table 3).

In general, a shoulder and/or several weak bands are visible between 1650-1700 $cm^{-1}$, both by FTIR and Raman. These are either due to ν(C=O) of the carbonyl involved in H-bond interactions, or to Fermi resonance interactions between this

strong ν(C=O) band and overtones or combination modes from the signals around 800 $cm^{-1}$ (Fig. S1 (Supplementary material), Table 3).

For DAID, the strongest infrared band (weak in Raman) occurs at 1632 $cm^{-1}$, while for GEN an intense broad ν(C=O) feature is observed at 1652 $cm^{-1}$ (Fig. S1). In turn, the DAID strongest Raman band is detected at 1619 $cm^{-1}$ (Fig. S1) and the same vibrational mode seems to contribute to the strong infrared signal also assigned to ν($C^4O^{12}$) (Table 3). For GEN, the most intense Raman feature is found at 1615 $cm^{-1}$ (Fig. S1) comprising a contribution from ν($C^4O^{12}$), in good agreement with the fairly intense infrared band at 1616 $cm^{-1}$ (Table 3).

In contrast to DAID and GEN, FOR displays four strong FTIR bands with similar intensities between 1550 and 1650 $cm^{-1}$ (Fig. S1), the one at higher frequency (1639 $cm^{-1}$) being assigned to ν(C=O) (Table 3). Figure S2 (Supplementary material) represents the experimental and calculated FTIR spectra for the two most populated FOR conformations. Also for GEN, two signals are detected in the Raman spectrum, at 1582 and 1588 $cm^{-1}$, evidencing the presence of two different ($O^7H$) orientations in the solid state for this molecule (conformers 1 and 3, Table 1), in accordance with the DFT calculations (which predict different frequencies for this vibrational mode, Table 3).

Regarding the carbonyl stretching mode, the calculated wavenumbers follow a different trend from the experimental ones (Table 3). DAID and FOR, with no intramolecular H-bonds, display lower experimental frequencies than the predicted ones (Table 3), with larger differences between the calculated values for the isolated molecule and the experimental ones in the solid state certainly due to their involvement in intermolecular H-bond interactions in the latter (not considered by the calculations). Conversely, the strongly favoured (C=)O···H($O^5$) intramolecular

interaction that takes place in GEN possibly overrules the intermolecular H-bonds even in the condensed phase, which is reflected by the better agreement between calculated and experimental data for this compound.

*3.2.3. The 1550-1000 cm$^{-1}$ region*

The hydroxylated isoflavones presently studied display vibrational bands associated to δ(OH) modes mixed with ν(C=O), ν(CC) and aromatic ring deformations, in the interval between 1550-1000 cm$^{-1}$. These signals can yield reliable information on the relative orientation of the hydroxylic groups.

The FTIR spectra of DAID and FOR have similar patterns, with special emphasis for the pair of bands between 1450 and 1520 cm$^{-1}$, whereas for GEN a distinct spectral profile is observed, namely the signals at 1504 and 1520 cm$^{-1}$ (Table 3, Fig. S1). For DAID, infrared and Raman bands at 1450 and 1461 cm$^{-1}$ are probably due to the presence of distinct conformers displaying a *syn* orientation of the ($O^{4'}H$) hydroxylic group. Furthermore, the strong FTIR bands at 1239 and 1246 cm$^{-1}$ in DAID and FOR, respectively, display a shoulder, while the GEN feature at 1202 cm$^{-1}$ is clearly broadened (Fig. 3). This fact, coupled to the appearance of two weak infrared features for FOR and DAID around 1300 cm$^{-1}$ (Fig. 3) can only be explained by the occurrence of distinct conformations, even in the solid state (Table 1). In general, it may be concluded that there is spectral evidence of the coexistence of distinct orientations of the ($O^{7}H$) group in these compounds, yielding different conformations (possibly two) at room temperature.

*3.2.4. The region below 1000 cm$^{-1}$*

Below 1000 cm$^{-1}$, the out-of-plane modes – either deformations of the aromatic rings or out-of-plane bendings from the (CH) and (OH) oscillators – give rise to

strong infrared bands, while the corresponding Raman features are generally undetectable, the in-plane modes tending to be more Raman active.

Broad features or sets of superimposed infrared bands were observed in this spectral interval, mainly for GEN (Figs. 2 and 3). This pattern is probably due to combination between out-of-plane and in-plane modes – broad feature at about 730, 740 or 745 $cm^{-1}$ respectively for DAID, FOR and GEN (Table 3, Fig. 3). Meanwhile, narrow Raman bands are detected, with variable intensities, in the 650-750 $cm^{-1}$ region. For GEN, another broad feature is clearly seen between 560 and 650 $cm^{-1}$ (Fig. 3), likely to be affected by the intramolecular $(C=)O\cdots H(O–C^5)$ bond as the vibrational modes predicted for this molecule are very sensitive to the presence of the six-membered intramolecular ring due to this hydrogen close-contact.

Since the combination between in-plane and out-of-plane modes seems to be enhanced by a deviation from planarity, displayed by isoflavones (and predicted by DFT calculations), these bands are more clearly observed in these compounds than for previously studied flavones (unpublished results), which exhibit planar geometries.

## 4. Conclusions

A conformational analysis of a series of hydroxylated isoflavones was carried out, by optical vibrational spectroscopy (FTIR and Raman) coupled to theoretical approaches. The DFT calculations allowed the assessment of the conformational preferences of the compounds, strongly dependent on their intramolecular H-bonding profile, mainly when a hydroxyl group is present at position $C^5$ (GEN).

GEN is the only molecule from those investigated containing a $C^5$–OH group, involved in a strong intramolecular interaction which leads to the formation of a 6-membered intramolecular ring essential for geometrical stability. The presence of this

close contact has been clearly identified by FTIR, through the profile of the corresponding ν(OH) modes.

In addition, low frequency deviations of some of the ν(OH) bands detected for the presently studied compounds evidence the involvement of these hydroxyl groups in intermolecular interactions in the solid state, which affects the electronic delocalisation in this type of chromone derivatives.

Isoflavones, displaying a phenyl substituent in position $C^3$, are favoured as non-planar geometries due to the steric hindrance between the phenolic hydrogens and the H atom from the heterocyclic ring ($H^2$). This behaviour, theoretically predicted for the isolated molecules, is in good agreement with the crystallographic data available for similar chemical systems.

For the phenol-containing systems DAID and GEN, both hydroxyl groups (from the B-ring and at position $C^7$) tend to display an *anti* orientation relative to the pyrone ring. Furthermore, in DAID and FOR the rotation around the $C^7$–OH bond, the hydroxyl group assuming either an *anti* or a *syn* conformation, is associated to a very small energy gap (0.22 $kJ.mol^{-1}$): this is evidenced by the large number of bands detected for these compounds, which can only be justified by the presence of these two almost equally populated conformers.

In sum, special attention should be paid to the close relationship between structure and activity for these hydroxylated isoflavone derivatives, in view of attaining a better understanding of their well-recognised antioxidant properties (which have been evaluated by the authors in a parallel study) [29]. Only a detailed knowledge of the conformational behaviour of this group of phytochemicals will allow a rational design of optimised chemopreventive isoflavone-based agents, with improved efficacy and safety.

***Acknowledgments***

The authors thank financial support from the Portuguese Foundation for Science and Technology – PEst-OE/QUI/UI0070/2011 and PhD grant SFRH/BD/40235/2007 (NFLM). The Chemistry Department of the University of Aveiro is acknowledged for use of the FT-Raman spectrometer.

**References**

[1] C. Kaur, H. C. Kapoor, Int. J. Food Sci. Tech. 36 (2001) 703-725.

[2] O. Blokhina, E. Virolainen, K. V. Fagerstedt, Ann. Bot. 91 (2003) 179-194.

[3] E. Riboli, T. Norat, Am. J. Clin. Nutr. 78 (2003) 559S-69S.

[4] L. Bravo, Nutr. Rev. 56 (1998) 317-33.

[5] P. G. Pietta, J. Nat. Prod. 63 (2000) 1035-42.

[6] P. van't Veer, M. C. Jansen, M. Klerk, F. J. Kok, Public Health Nutr. 3 (2000) 103-7.

[7] C. G. Heijnen, G. R. Haenen, F. A. van Acker, W. J. van der Vijgh, A. Bast, Toxicol. in Vitro 15 (2001) 3-6.

[8] C. A. Gomes, T. G. da Cruz, J. L. Andrade, N. Milhazes, F. Borges, M. P. Marques, J. Med. Chem. 46 (2003) 5395-401.

[9] W. Ren, Z. Qiao, H. Wang, L. Zhu, L. Zhang, Med. Res. Rev. 23 (2003) 519-34.

[10] Y. J. Surh, Nat. Rev. Cancer 3 (2003) 768-80.

[11] T. J. Key, A. Schatzkin, W. C. Willett, N. E. Allen, E. A. Spencer, R. C. Travis, Public Health Nutr. 7 (2004) 187-200.

[12] B. A. Graf, P. E. Milbury, J. B. Blumberg, J. Med. Food 8 (2005) 281-90.

[13] P. Fresco, F. Borges, C. Diniz, M. P. Marques, Med .Res. Rev. 26 (2006) 747-66.

[14] B. Swinburn, Public Health Nutr. 12 (2009) 877-8.

[15] P. Fresco, F. Borges, M. Marques, C. Diniz, Curr. Pharm. Design 16 (2010) 114-34.

[16] G. Mandalari, R. M. Faulks, C. Bisignano, K. W. Waldron, A. Narbad, M. S. Wickham, FEMS Microbiol. Lett. 304 (2010) 116-22.

[17] C. J. Dillard, J. B. German, J. Sci. Food Agric. 80 (2000) 1744-56.

[18] E. Middleton, Jr., C. Kandaswami, T. C. Theoharides, Pharmacol. Rev. 52 (2000) 673-751.

[19] B. H. Havsteen, Pharmacol. Ther. 96 (2002) 67-202.

[20] M. A. Soobrattee, V. S. Neergheen, A. Luximon-Ramma, O. I. Aruoma, T. Bahorun, Mutat. Res. Fund. Mol. 579 (2005) 200-13.

[21] E. Haslam, Practical Polyphenolics : from Structure to Molecular Recognition and Physiological Action. Cambridge University Press, Cambridge, 1998.

[22] H. Fang, W. D. Tong, L. M. Shi, R. Blair, R. Perkins, W. Branham, B. S. Hass, Q. Xie, S. L. Dial, C. L. Moland, D. M. Sheehan, Chem. Res. Toxicol. 14 (2001) 280-294.

[23] E. S. Manas, Z. B. Xu, R. J. Unwalla, W. S. Somers, Structure 12 (2004) 2197-2207.

[24] N. F. Machado, M. P. Marques, Curr. Bioact. Comp. 6 (2010) 76-89.

[25] H.-Q. Li, J.-Y. Xue, L. Shi, S.-Y. Gui, H.-L. Zhu, Eur. J. Med. Chem. 43 (2008) 662-667.

[26] M. Lopez-Lazaro, Curr. Med. Chem. - Anti-Cancer Agents 2 (2002) 691-714.

[27] K. E. Heim, A. R. Tagliaferro, D. J. Bobilya, J. Nutr. Biochem. 13 (2002) 572-584.

[28] A. Seyoum, K. Asres, F. K. El-Fiky, Phytochem. 67 (2006) 2058-70.

[29] M. M. Dias, N. F. L. Machado, M. P. M. Marques, Food Funct. 2 (2011) 595-602.

[30] C.S. Young, H.T. Youl, A.J. Yun, K.S. Ran, K.K. Sun, H.I. Kyeong, K. Suna, Planta Medica 74 (2008) 25-32.

[31] V. Crupi, D. Majolino, A. Paciaroni, B. Rossi, R. Stancanelli, V. Venuti, G. Viliani, J. Raman Spectrosc. 41 (2010) 764-770.

[32] M. J. Frisch, G. W. Trucks, H. B. Schlegel, G. E. Scuseria, M. A. Robb, J. R. Cheeseman, J. J. A. Montgomery, T. Vreven, K. N. Kudin, J. C. Burant, J. M. I. Millam, S. S. , J. Tomasi, V. Barone, B. Mennucci, M. Cossi, G. Scalmani, N. Rega, G. A. Petersson, H. Nakatsuji, M. Hada, M. Ehara, K. Toyota, R. Fukuda, J. Hasegawa, M. Ishida, T. Nakajima, Y. Honda, O. Kitao, H. Nakai, M. Klene, X. Li, J. E. Knox, H. P. Hratchian, J. B. Cross, V. Bakken, C. Adamo, J. Jaramillo, R. Gomperts, R. E. Stratmann, O. Yazyev, A. J. Austin, R. Cammi, C. Pomelli, J. W. Ochterski, P. Y. Ayala, K. Morokuma, G. A. Voth, P. Salvador, J. J. Dannenberg, V. G. Zakrzewski, S. Dapprich, A. D. Daniels, M. C. Strain, O. Farkas, D. K. Malick, A. D. Rabuck, K. Raghavachari, J. B. Foresman, J. V. Ortiz, Q. Cui, A. G. Baboul, S. Clifford, J. Cioslowski, B. B. Stefanov, G. Liu, A. Liashenko, P. Piskorz, I. Komaromi, R. L. Martin, D. J. Fox, T. Keith, M. A. Al-Laham, C. Y. Peng, A. Nanayakkara, M. Challacombe, P. M. W. Gill, B. Johnson, W. Chen, M. W. Wong, J. Gonzalez, J. A. Pople, Gaussian 03, Revision D.01, Gaussian Inc., Wallingford, CT, 2004.

[33] C. Lee, W. Yang, R. G. Parr, Phys. Rev. B 37 (1988) 785-789.

[34] B. Miehlich, A. Savin, H. Stoll, H. Preuss, Chem. Phys. Lett. 157 (1989) 200-206.

[35] A. D. Becke, Phys. Rev. A 38 (1988) 3098-3100.

[36] A. D. Becke, J. Chem. Phys. 98 (1993) 1372-1377.

[37] G. A. Petersson, A. Bennett, T. G. Tensfeldt, M. A. Allaham, W. A. Shirley, J. Mantzaris, J. Chem. Phys. 89 (1988) 2193-2218.

[38] C. Peng, P. Y. Ayala, H. B. Schlegel, M. J. Frisch, J. Comput. Chem. 17 (1996) 49-56.

[39] J. P. Merrick, D. Moran, L. Radom, J. Phys. Chem. A 111 (2007) 11683-11700.

[40] N. F. L. Machado, R. Valero, H. S. Domingos, J. Tomkinson, L. A. E. Batista de Carvalho, J. C. Otero, M. P. M. Marques, Vib. Spectrosc. 63 (2012) 325-337.

[41] D. Michalska, R. Wysokinski, Chem. Phys. Lett. 403 (2005) 211–217.

[42] S.I. Gorelsky, SWizard Program, University of Ottawa, Canada, 2010, http://www.sg-chem.net/.

[43] S.I. Gorelsky, A.B.P. Lever, J. Organomet. Chem. 635 (2001) 187–196.

[44] J. M. Petrosky, C. De Sa Valente, E. P. Kelson, S. Collins, J. Phys. Chem. A 106 (2002) 11714-11718.

[45] A. P. Mazurek, L. Kozerski, J. Sadlej, R. Kawe, E. Bednarek, J. Sitkowski, J. Cz. Dobrowolski, J. K. Maurin, K. Biniecki, J. Witowska, P. Fiedor, J. Pachecka, J. Chem. Soc., Perkin Trans. 2 (1998) 1223-1230.

[46] Q.-Y. Wang, Acta Crystallogr. E 64 (2008) o893.

[47] H.M. Ishiki, C. Aleman, S.E. Galembeck, Chem. Phys. Lett. 287 (1998) 579-584.

[48] R. Sekine, J. Vongsvivut, E. G. Robertson, L. Spiccia, D. McNaughton, J. Phys. Chem. B 114 (2010) 7104-7111.

[49] R. Sekine, E. G. Robertson, D. McNaughton, Vib. Spectrosc. 57 (2011) 306-314.

[50] R. Sekine, J. Vongsvivut, E. G. Robertson, L. Spiccia, D. McNaughton, J. Phys. Chem. B 115 (2011) 13943-54.

[51] J. P. Cornard, L. Vrielynck, J. C. Merlin, J. C. Wallet, Spectrochim. Acta A 51 (1995) 913-923.

[52] R. D. H. Murray, P. H. Mccabe, Tetrahedron 25 (1969) 5819-5837; *ibid*, 5839-5851.

[53] E. B. Wilson, Phys. Rev. 45 (1934) 0706-0714.

**Figure captions**

Fig. 1. Calculated (B3LYP/6-31G**) lowest energy geometries for the isoflavone derivatives presently studied. (The atom numbering is included, as well as the possible intramolecular H-bonds (dashed lines) and repulsive interactions (dotted lines). Distances are in pm. ! represents the ($C^2C^3C^{1'}C^{6'}$) dihedral).

Fig. 2. Experimental (solid line) and calculated (B3LYP/6-31G**, dotted line) Raman spectra (100-1900 $cm^{-1}$ and 2800-3600 $cm^{-1}$) for the presently studied isoflavones.

Fig. 3. Experimental (solid line) and calculated (B3LYP/6-31G**, dotted line) FTIR spectra (400-1800 $cm^{-1}$) and (2000-3750 $cm^{-1}$) for the presently studied isoflavones.

**Highlights:**

- Full vibrational assignment of a series of dietary hydroxylated isoflavones

- Complete conformational analysis

- Use of vibrational spectroscopy for establishing reliable structure-activity relationships (SAR´s)

- SAR´s will allow to understand the health-promoting ability of dietary compounds (phytochemicals)

Table 1 Most stable conformers calculated for the substituted isoflavones under study.

| Compound | | [c]Conformational description (dihedral values) | | | | |
|---|---|---|---|---|---|---|
| [a]ΔE | [b]pop. | $C^2C^3C^{1'}C^{6'}$ | $C^6C^5OH$ | $C^8C^7OH$ | $C^{3'}C^{4'}OH$ | $C^{3'}C^{4'}O(CH_3)$ |
| DAID | | - | | | | |
| 0.00 | 31.3% | 142.5 | - | 180.0 | -178.7 | - |
| 0.22 | 28.6% | 142.5 | - | 0.1 | -178.5 | - |
| 0.95 | 21.3% | 141.4 | - | -179.9 | 0.0 | - |
| 1.27 | 18.7% | 141.3 | - | 0.0 | 0.0 | - |
| FOR | | - | | | | |
| 0.00 | 29.5% | 142.7 | - | 180.0 | - | -178.8 |
| 0.22 | 27.0% | 142.7 | - | 0.1 | - | -178.8 |
| 0.61 | 23.0% | 141.2 | - | -179.9 | - | 0.2 |
| 0.91 | 20.4% | 141.2 | - | 0.0 | - | 0.1 |
| GEN | | - | | | | |
| 0.00 | 40.5% | 141.3 | -179.9 | 180.0 | -178.7 | - |
| 0.83 | 28.9% | 140.2 | -179.9 | -179.9 | 0.0 | - |
| 1.99 | 18.2% | 141.3 | -179.8 | 0.1 | -178.6 | - |
| 2.92 | 12.5% | 141.1 | -179.8 | 0.0 | -0.1 | - |

[a]Energy differences in $kJ.mol^{-1}$ calculated at the B3LYP/6-31G** level. [b]Boltzmann distribution at room temperature, based on the B3LYP/6-31G** electronic energy corrected by the zero-point vibrational value (obtained at the same level of theory). [c]In degrees. The atoms are labelled according to Fig. 1.

e 2 - Comparison between X-Ray crystallographic structures and the presently calculated ones.

| tructural rameter | [b]Solid | | [c]Calculated | | |
|---|---|---|---|---|---|
| | GMC | EFOR | DAID | GEN | FOR |
| $^{4}=O^{12}$ | 126.3 | 123.1 | 123.2 | 125.2 | 123.2 |
| $^{2}=C^{3}$ | 133.8 | 134.6 | 135.7 | 135.8 | 135.7 |
| [d]C---C | 139.7 | 138.6 | 139.8 | 140.3 | 139.8 |
| $C^{3}C^{1'}$ | 148.2 | 148.5 | 148.1 | 148.1 | 148.1 |
| $C^{5}O$ | 139.5 | - | - | 133.6 | - |
| $C^{4'}O$ | 136.0 | 137.9 | 136.6 | 136.5 | 136.5 |
| H···O=C | 165.2 | - | - | 165.6 | - |
| H···$O^{12}$ (º) | 153.6 | - | - | 150.3 | - |
| $O^{1}C^{2}$ (º) | 119.4 | 118.5 | 118.8 | 119.5 | 118.8 |
| **ψ** (º) | 116.2 | 137.0 | 142.5 | 141.3 | 142.7 |

ces in pm; Ψ values in degrees. The atoms are labelled according to Fig. 1. [b]Values d from X-ray crystallography [42,43] [c]Calculated at the B3LYP/6-31G** level, for the energy conformations. [d]Distance corresponding to the average of the six bond-lenghts e aromatic A-ring.

· Experimental solid state Raman (NR), FTIR and calculated wavenumbers ($cm^{-1}$) for DAID, GEN and FOR.

| Experimental | | | | | Calculated[a] | | | Assignment[b] |
|---|---|---|---|---|---|---|---|---|
| | GEN | | FOR | | DAID | GEN | FOR | |
| TIR | NR | FTIR | NR | FTIR | | | | |
| | 3410 | ~3450 | | | | 3656 | | $\nu(O^{4'}H)^B$ |
| | | 3410 | | 3130 | 3657 | 3655 | 3656 | $\nu(O^7H)$ |
| 200 | | | | | 3656 | | | $\nu(O^{4'}H)^B$ |
| 115 | 3103 | 3104 | 3100 | | 3105 | 3105 | 3104 | $\nu(CH)^B + \nu(C^8H)^c$ |
| 084 | 3082 | 3086 | 3082 | | 3095 | 3101 | | |
| | | | | 3078 | 3094 | 3097 | 3095 | $\nu(C^2H) + \nu(C^8H) + (\nu(CH)^B)^c$ |
| | | | 3073 | | | | 3081 | |
| | | | | | | | 3073 | $\nu(CH)^{A,B}$ |
| | 3058 | 3050 | | | | 3060 | | |
| | | | | | | 3055 | | $\nu(CH)^B + \nu(C^6H)$ |
| 040 | | | | | 3038 | | | $\nu(C^6H)$ |
| 023 | 3023 | | 2993 | 2993 | 3029 | 3030 | 3047 | $\nu(CH)^B$ |
| | | | 2980 | 2981 | | | 3038 | $\nu(CH)^A$ |
| | | | 2952 | 2952 | | | 3013 | $\nu_{as}(CH_3)$ |
| | | | 2899 | 2900 | | | 2947 | $\nu_{as}(CH_3)$ |
| | | | 2835 | 2836 | | | 2886 | $\nu_s(CH_3)$ |
| | | ~2500-3300 | | | | 3038 | | $\nu(O^5H)$ |
| 570 | 1657 | | 1660 | 1660 | | | | FR |
| 532 | 1646 | 1652 | 1638 | 1639 | 1664 | 1644 | 1664 | $\nu(C{=}O) + ((\phi 8a/b)^A + \delta(O^5H))^c$ |
| | | | | 1620 | 1612 | 1607 | 1612 | $\phi 8a^A + (\phi 8a^B)^c$ |
| 507 | 1615 | 1616 | 1620 | 1609 | 1607 | 1606 | 1604 | $\phi 8a^B + ((\phi 8a/b)^A + \nu(C^2C^3) + \nu(C{=}O))^c$ |
| | 1588 | | | | | 1587[d] | | $\nu(C^2C^3) + \nu(C{=}O) + \delta(OH)^A$ |
| 596 | 1582 | 1584 | 1596 | 1596 | 1599 | 1584 | 1599 | $\nu(C^2C^3) + (\nu(C{=}O) + \delta(OH)^A)^c$ |
| | | 1571 | 1581 | 1580 | 1674 | 1575 | 1562 | $(\phi 8a/8b + \delta(OH))^{B/A}$ |
| | 1568 | 1553 | 1569 | 1569 | 1557 | 1563 | 1553 | $(\phi 8a/8b + \delta(OH))^{A/B} + \nu(C^2C^3)$ |
| 519 | 1515 | 1520 | 1513 | 1513 | 1536 | 1539 | 1537 | $\phi 19a^B + (\phi_{ip}{}^A + \delta(O^5H))^c$ |
| | 1502 | 1504 | | | | 1529 | | $\delta(O^5H) + \phi 19a^A + \phi 19a^B$ |
| 461 | | | | | 1481[e] | | | $(\phi 19b + \delta(OH))^A$ |
| 451 | 1468 | 1474 | 1455 | 1452 | 1476 | 1482 | 1476 | $(\phi 19b + \delta(OH))^A$ |
| | | | | | | 1415 | | $(\phi 14 + \delta(OH))^A + \nu(C^3C^4) + \nu(O^1C^2) + \phi_{ip}{}^B$ |
| | 1397 | 1397 | | | | 1381 | | $\delta(C^2H) + \nu(C^3C^4) + \phi_{ip}{}^A$ |
| | 1317 | 1317 | | | | 1342 | | $\delta(C^2H) + (\phi 14/3)^A + \delta(O^5H)$ |
| 308 | | | 1318 | 1318 | 1315[e] | | 1314[e] | $(\phi_{ip} + \upsilon(C^7O))^A + \delta(C^2H) + \nu(C^3Ph)$ |
| | 1307 | 1310 | | | | 1327 | | $\phi_{ip}{}^A + \delta(C^2H) + \delta(O^5H) + \nu(C^3Ph)$ |
| 296 | | | | 1310 | 1308 | | 1307 | $(\phi_{ip} + \nu(C^7O))^A + \delta(C^2H) + \nu(C^3Ph)$ |
| 280 | 1282 | 1275 | 1279 | 1274 | 1292 | 1293 | 1280 | $(\phi 18b + \nu(C^{4'}O))^B + \upsilon(C^3Ph) + r(CH_3)^f$ |
| | 1262 | | | | | 1273 | | $\nu(O^1C^2) + \nu(C^3Ph) + \phi 18a^B + \phi_{ip}{}^A + \delta(OH)^A$ |
| 252 | | | 1261 | 1252 | 1277 | | 1277 | $(\phi_{ip} + \delta(OH))^A + \nu(C_3Ph) + \phi 18a^B + \nu(C^7O) + \nu(C^{4a}C^4)$ |
| | | 1259 | | | | 1245 | | $(\phi_{ip} + \nu(CO))^A + \delta(O^7H)$ |
| 239 | | | 1248 | 1246 | 1272[e] | | 1272[e] | $(\phi_{ip} + \delta(OH))^A + \nu(C^3Ph) + \phi 18a^B + \nu(C^7O) + \nu(C^{4a}C^4)$ |
| | | | 1217 | 1220 | 1234 | | 1234 | $\phi 9b^A + \nu(O^1C^2) + \nu(C^3Ph) + \phi_{ip}{}^B$ |
| | | 1210 | | | | 1212 | | $\nu(O^1C^2) + \nu(C^4C^{4a}) + (\phi_{ip} + \delta(O^5H))^A$ |
| | 1200 | 1202 | | | | 1209[d] | | $\nu(O^1C^2) + \nu(C^4C^{4a}) + (\phi_{ip} + \delta(O^5H))^A$ |
| 193 | | | 1196 | 1195 | 1215 | | 1215 | $(\phi 9a/12 + \delta(OH))^A + \nu(O^1C^2) + \nu(C^{4a}C^4)$ |
| | 1184 | 1180 | | | | 1187 | | $\delta(O^7H) + \delta(C^6H) + (\phi 9a/b)^B$ |
| 172 | 1178 | 1172 | 1180 | 1179 | 1189 | 1180 | 1194 | $\phi 9a^B + r(CH_3)^f + \delta(O^{4'}H)^g$ |
| | 1145 | 1149 | | | | 1155 | | $\delta(C^6H) + \nu(C^7O) + \delta(O^7H) + \phi_{ip}{}^A$ |
| 89 | 885 | 886 | 888 | 888 | 887 | 883 | 886 | $\Delta(C^2C^3C^4) + \phi 1^B + \phi_{ip}{}^A$ |
| 91 | 789 | 791 | | | 781 | 783 | | $\phi_{ip}{}^A + \Delta(C^{8a}O^1C^2) + \phi_{oop}{}^B / \Gamma(C^{4a}C^4C^3) + \phi_{oop}{}^{A/B} + \gamma(O^5H)^c$ |
| 34 | | 745 | | 742 | 769 | 766 | 773 | $\Gamma(C^{4a}C^4C^3) + \phi_{oop}{}^{A/B} + \gamma(O^5H)^a / \phi_{ip}{}^A + \Delta(C^{8a}O^1C^2) + \phi_{oop}{}^B$ |
| 25 | 727 | 728 | 730 | 732<br>719 | 734 | | 734 | $\phi 6a^A$ |
| 92 | 702 | 705 | 694 | 693 | 716 | 716 | 720 | $\phi 4^B$ |
| | | | 641 | 643 | 647 | | 646 | $(\phi 6a/6b)^B$ |
| 27 | | | 625 | 624 | 624 | | 622 | $(\phi 6a/6b + \Delta(C^{4'}OC))^B + \Delta(C^{8a}O^1C^2) / \phi 16a^B$ |
| | 622 | 620 | | | | 619 | | $\phi 16a^A / \phi_{ip}{}^{A/B} + \Delta(C^3C^4O^{12})$ |
| | 613 | 607 | | | | 615 | | $\phi_{ip}{}^{A/B} + \Delta(C^3C^4O^{12}) / \phi 16a^A$ |
| | 590 | 591 | | | | 592 | | $\phi_{ip}{}^A$ |
| | | 567 | | | | 565 | | $(\phi_{ip} + \Delta(COH))^A + \Delta(C^3C^4O^{12}) / \phi_{oop}{}^B$ |
| 47 | 559 | | 551 | 552 | 547 | | 551 | $\Delta(C^3C^4C^{4a}) + \Delta(C^2O^1C^{8a}) + \Delta(COH)^A$ |
| 29 | | | 531 | 532 | 534 | 533 | 541 | $\phi_{oop}{}^B / (\phi_{ip} + \Delta(COH))^A + \Delta(C^3C^4O^{12})$ |
| | 530 | 534 | | | | 512 | | $(\phi_{ip} + \Delta(COH))^A + \Delta(C^3C^4C^{4a}) + \Delta(C^2O^1C^{8a})$ |

'P/6-31G** level; scaled wavenumbers [39,40] (see experimental section). For clarity sake, not all the predicted modes are included – only relate with the observed bands. [b]Atoms are numbered according to Fig. 1. The Wilson notation was used for the description of the aromatic ring ions (ϕ) [53]. $\delta$ – in-plane deformation, $r$ – rocking, γ – out-of-plane deformation, Γ – out-of-plane deformation , Δ – in-plane deformation of as, iph – in-phase, ooph – out-of-phase, ip – in-plane, oop – out-of-plane; the subscripts *as* and *s* refer to anti-symmetric or symmetric modes, FR represents a Fermi resonance. The superscripts A and B refer to rings A and B, respectively (Fig. 1); Ph refers to the entire phenyl ring. [f,g]Refer to components of a vibrational mode exclusive to GEN, FOR, and DAID, respectively. [d]For conformer 3. [e]For is substituents. [c,f,g]

Figure 1 B&W

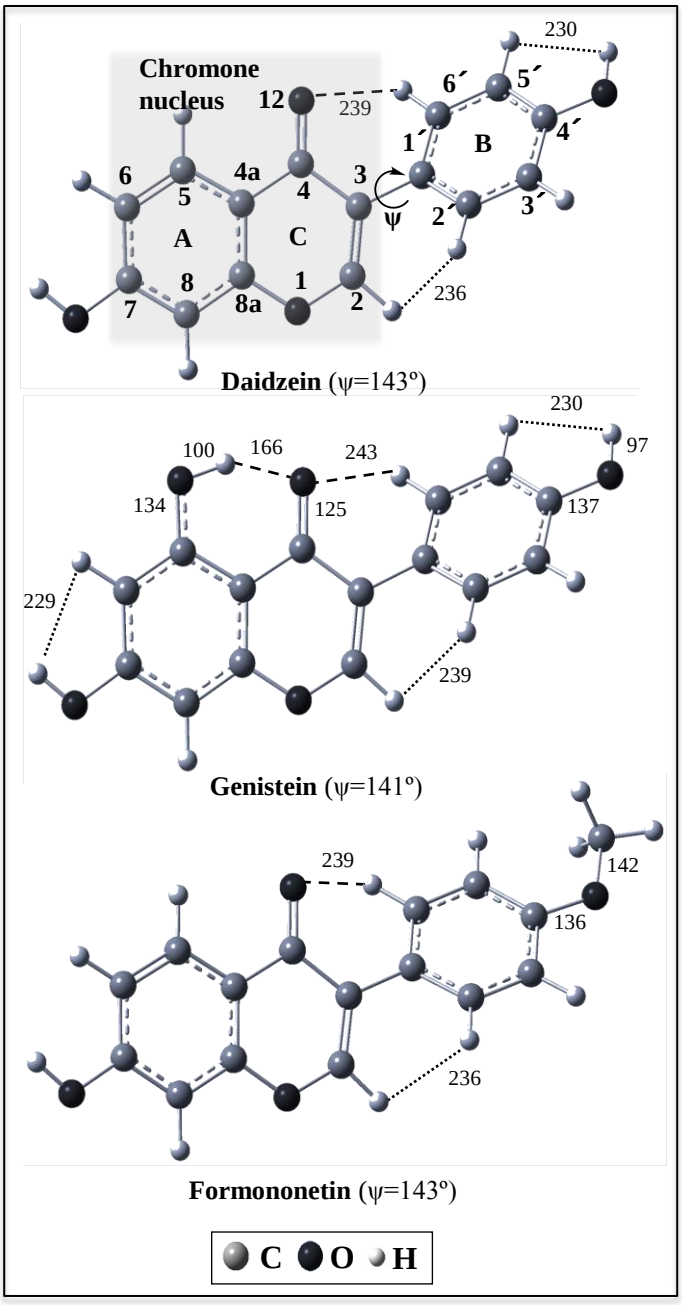


**Fig. 1**

Figure 1 colour

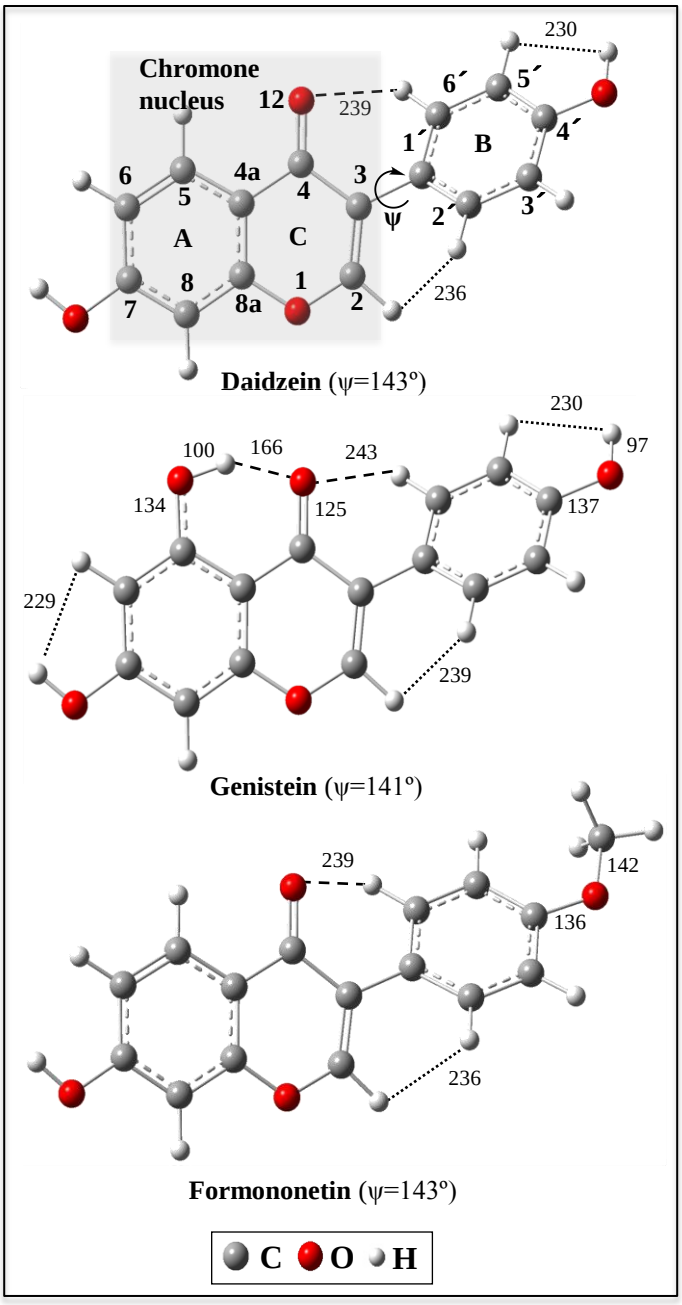


**Fig. 1**

Figure 2

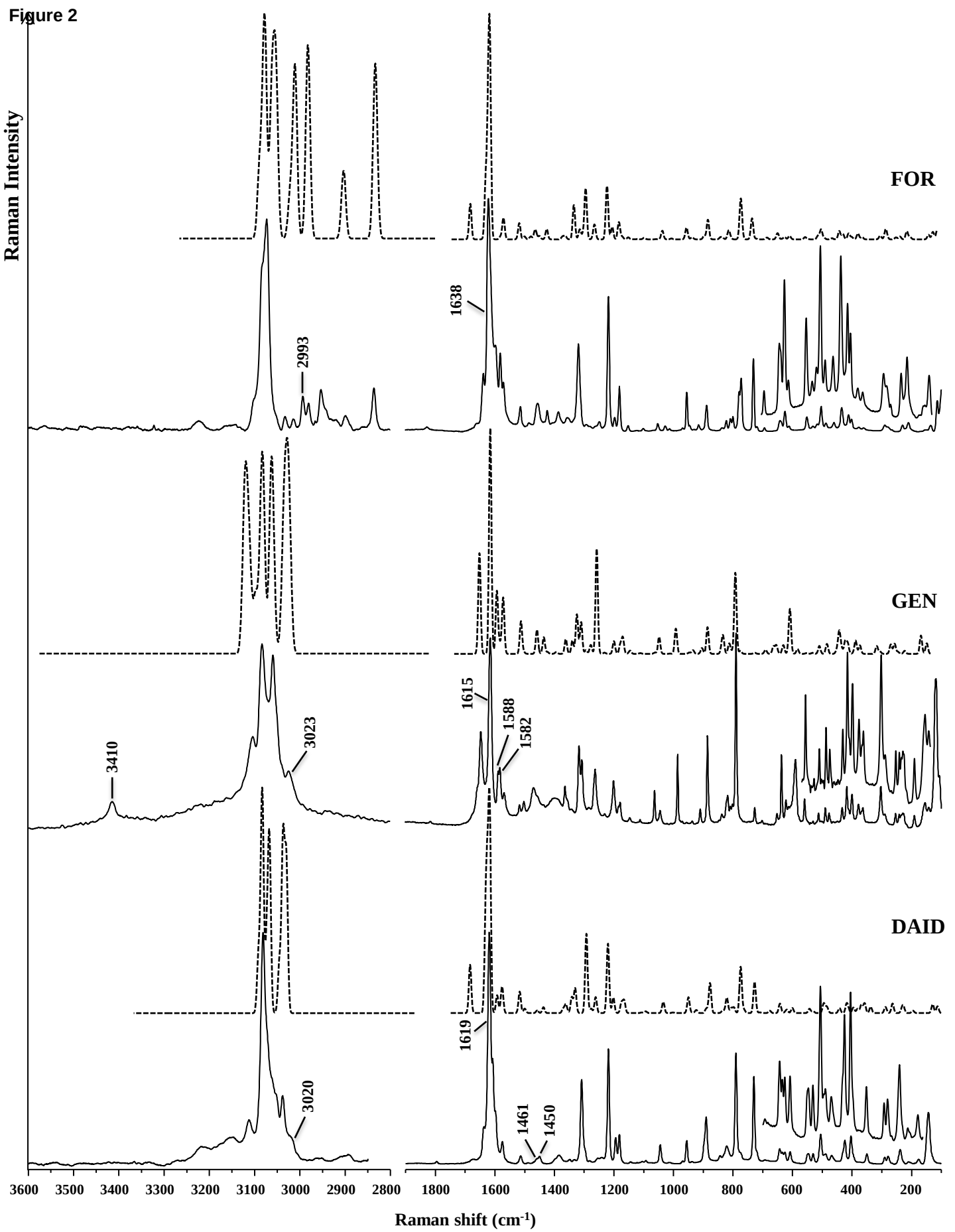


**Fig. 2**

Figure 3

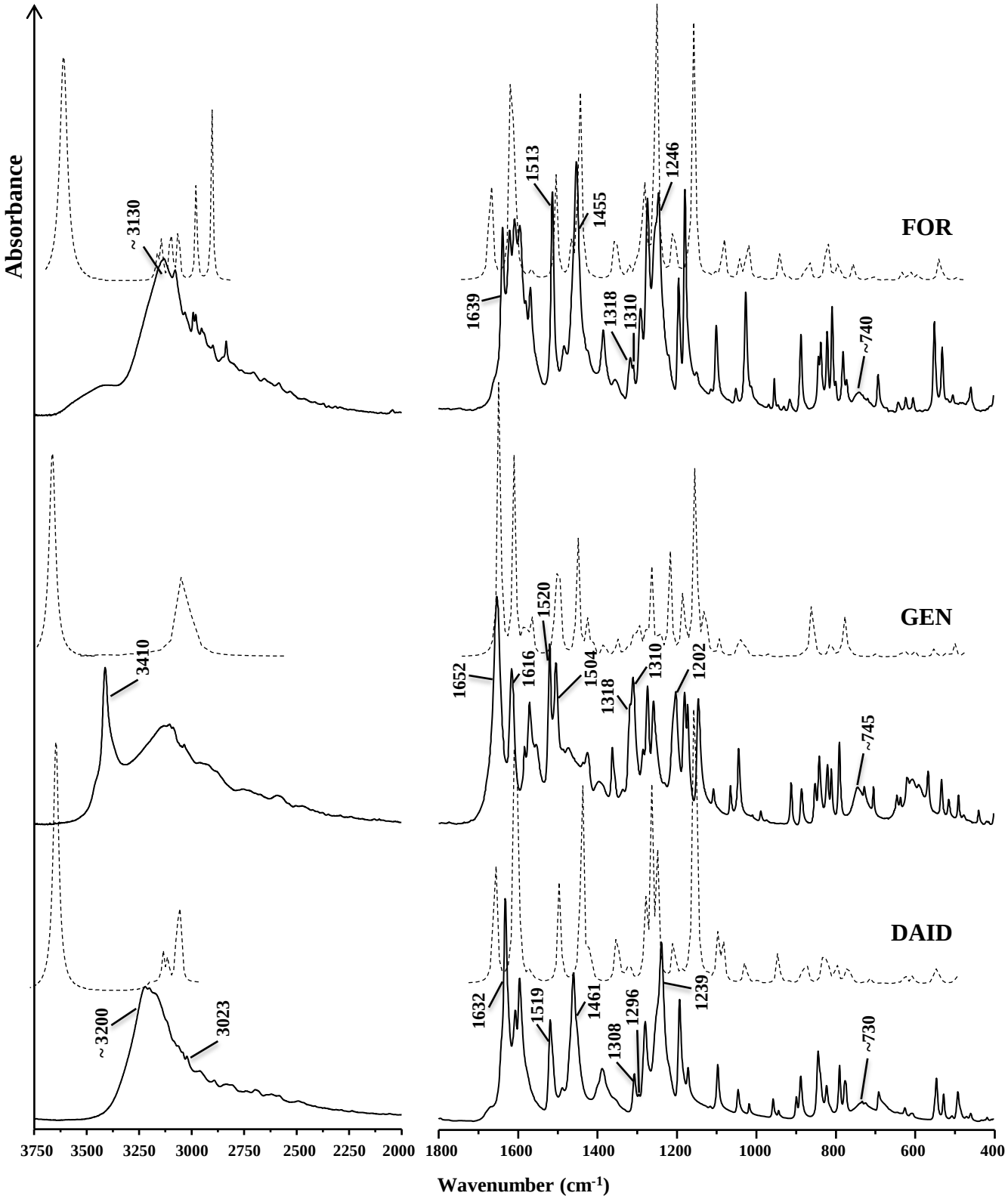


**Fig. 3**

**Highlights:**

- Full vibrational assignment of a series of dietary hydroxylated isoflavones

- Complete conformational analysis

- Use of vibrational spectroscopy for establishing reliable structure-activity relationships (SAR´s)

- SAR´s will allow to understand the health-promoting ability of dietary compounds (phytochemicals)

**Graphical abstract**

# Table of contents

**A Conformational Study of Hydroxylated Isoflavones by Vibrational Spectroscopy Coupled to DFT Calculations**

N.F.L. Machado, L.A. E. Batista de Carvalho
J.C. Otero and M.P.M. Marques

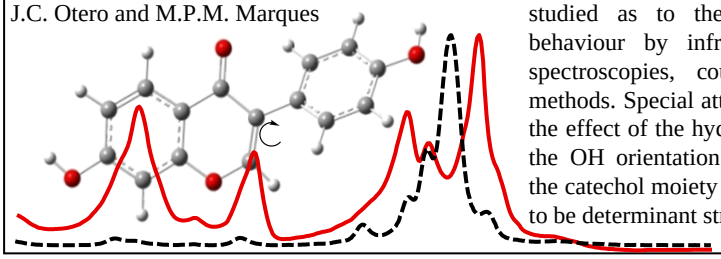

Dietary hydroxylated isoflavones were studied as to their conformational behaviour by infrared and Raman spectroscopies, coupled with DFT methods. Special attention was paid to the effect of the hydroxyl substitution, the OH orientation at $C^7$ and within the catechol moiety having been found to be determinant structural factors.